Introducción de un factor de mapa Mercator variable en la formulación espectral del modelo HARMONIE

Introduction of a variable Mercator map factor in the spectral part at the HARMONIE model

Isabel MARTÍNEZ-MARCO & Inés SANTOS-ATIENZA

Área de Modelización Numérica del Tiempo
Agencia Estatal de Meteorología (AEMET), Spain
i.martinez@inm.es

RESUMEN

Se ha codificado una nueva formulación del cálculo espectral en el modelo HARMONIE para grandes dominios. Dicha formulación utiliza la proyección Mercator rotada y su factor de mapa representado por una combinación lineal de armónicos de Fourier. El modelo de referencia emplea el valor máximo de dicho factor de mapa sobre todo el área. La mejora, entre usar la aproximación de Fourier o el valor máximo del factor de mapa, aumenta con el tamaño del dominio de integración. En la parte espectral, se han introducido tres coeficientes de la serie de cosenos de Fourier mediante el uso de una matriz multidiagonal simple. Se muestran los primeros resultados de estas modificaciones en integraciones semi-Lagrangianas con largos pasos de tiempo.

Palabras clave: Predicción numérica del tiempo; métodos semi-Lagrangianos; modelos espectrales; factor de mapa Mercator; series de Fourier

ABSTRACT

For large domains, a new formulation of the spectral computation has been implemented in the HARMONIE model. The formulation makes use of the rotated/tilted Mercator projection and of its map factor represented by a linear combination of low-order Fourier harmonics. The reference model uses the maximum value of the map factor over the whole area. The improvement between using the Fourier approximation or the maximum value of the map factor increases with the size of the integration domain. In the spectral part, three coefficients of the Fourier cosine series have been introduced through a simple diagonal multiplicative operator. The first results of these modifications are presented for semi-Lagrangian integrations with long time-steps.

Key words: Numerical weather prediction; semi-Lagrangian methods; spectral models; Mercator map factor; Fourier series

1. INTRODUCTION

The HARMONIE (Hirlam Aladin Regional/Meso-scale Operational NWP In Europe) model is being developed since 2005 as a cooperative project between ALADIN and HIRLAM consortia and will be used operationally for Numerical Weather Prediction (NWP). Its main characteristics are a spectral horizontal formulation with a bi-Fourier function basis, a hydrostatic-pressure hybrid vertical coordinate and a non-hydrostatic dynamical kernel.

The HARMONIE model works in a projected geometry: the spectral part of the equations is written in the transformed coordinate system while the grid-point part is treated in the geographical coordinate system.The choice of a conformal geometrical transformation leads to a very simple relationship between the rescaled first-order differential operator $\vec{\nabla}'$ and its geographical counterpart $\vec{\nabla}$:

$$\vec{\nabla} = M\,\vec{\nabla}'$$

where M denotes the map factor (distance on the transformed sphere/distance on the geographical sphere) at the considered location.

In the semi-implicit scheme of the ALADIN model, the value of the map factor is a constant equal to its maximum value over the integration domain (Bénard, 2003). This simplification seems to be legitimate for limited area models used in small domains, in which the map factor remains close to the unity. However, the HARMONIE community leads towards the use of large domains and, in this case, its values are greater than the unity. Thus, from the stability point of view, the variability of this factor over the integration domain should be considered.

Yessad and Bénard (1996) make clear how to solve this problem at the ARPEGE global model by writing the map factor as a combination of Legendre polynomials of orders zero and one. In this case, the variations of the map factor are exactly and entirely included in the first component of the spectral formulation. The solution of the Helmholtz equation yielded by the model consists of the inversion of a pentadiagonal matrix for each zonal number and time-step.

In order to apply the same method to the HARMONIE model, the formulation of the map factor in this model should have a simple pattern at the spectral space: linear combination of low-order Fourier harmonics. Consequently, the mapping factor dependency in the spectral part of the computations can be included by a simple extra multi-diagonal multiplicative operator. This expression should improve the behaviour of the model when increasing the integration domain and, at the same time, the extra computation and memory cost should be small. An inconvenient of

using this method is the requisite of knowing the mapping factor analytic form for the different projections in the bi-Fourier spectral space (Voitus, 2004).

The aim of this paper is to show the analytical expression of the Mercator map factor expanded as a Fourier series, to study the behaviour of this Fourier approximation and to include it in the HARMONIE model. First, as starting point of this study, the general expression of this map factor is presented. Second, the authors have expanded this expression as a Fourier series and calculated its coefficients analytically. In this way, the inconvenient explained previously is removed, allowing their implementation in the HARMONIE model for the rotated Mercator projection. Third, several comparative studies for different sizes of the integration domain are showed. Fourth, first results with the new semi-implicit scheme are presented and compared to the reference one. Finally, a short conclusion of these points is given.

2. THE MERCATOR MAP FACTOR

For a Mercator projection, the expression of its map factor m in spherical coordinates is:

$$m(\lambda, \varphi) = \frac{1}{cos(\varphi)},$$

where φ is the latitude and λ is the longitude. In cartesian coordinates (x, y) of the plane:

$$m(x, y) = m(y) = cosh(y/a),$$

where a is the radius of the Earth and $y \in [-\frac{L_y}{2}, \frac{L_y}{2}]$. We define L_y as the product of a factor f by the radius of the Earth, $a \cong 6371\,\text{km}$.

As it can be seen, this map factor depends on the latitude only.

Besides, let us say that the choice of the Mercator projection has been made on purpose, as its map factor expression (hyperbolic cosine) is one of the best suited for developing a Fourier cosine series (Bénard, 2004).

3. FOURIER COEFFICIENTS OF THE MERCATOR MAP FACTOR

Taking into account that the term which appears at the discrete equations of the model (Bénard, 2003) is the square of the map factor m^2, the Fourier series coefficients calculated are the first ones of this even function belonging to $L^2[-\frac{L_y}{2}, \frac{L_y}{2}]$; where $[-\frac{L_y}{2}, \frac{L_y}{2}]$ is the domain considered. It is known that for any even function of L^2 in a bounded interval there is a Fourier cosine series

converging to the function in that interval. As it has been already said, m^2 fulfills these conditions. Consequently, there is a Fourier cosine series converging to m^2 in $L^2[-\frac{L_y}{2}, \frac{L_y}{2}]$. To be precise,

$$m^2(y) = \frac{1}{2}a_0 + \sum_{n=1}^{\infty} a_n cos(\frac{2\pi n}{L_y}y)dy,$$

with

$$a_n = \frac{4}{L_y} \int_0^{\frac{L_y}{2}} m^2(y) cos(\frac{2\pi n}{L_y}y)dy, \quad n = 0,1,2,...$$

These coefficients have been computated analytically by the authors. Because of space, the detailed development of this calculation is included in the Appendix. Its analytical computation provides the following values for the Fourier coefficients, depending on the parameter f:

$$a_0 = \frac{1}{2f}(e\,f - e^{-f}) + 1$$

$$a_n = \frac{(-1)^n f}{2[(\pi n)^2 + f^2]}(e^f - e^{-f}), \quad n = 1,2,...$$

4. NUMERICAL TESTS

Two types of test are carried out in this section. The first one shows the behaviour of the finite Fourier series of m^2 using different number of coefficients. The second one analyses the effect of the integration domain size considering the same Fourier truncation.

In the first test, two different comparisons are made. Figures 1a, 2a and 3a show the behaviour of the square map factor exact value, m^2, through the domain versus the Fourier truncations, $\hat{m}^2$. From these Figures, it can be seen that the more coefficients of the Fourier series are considered, the closer to the exact value the truncations are. Besides, it is remarkable the fact that the values of the map factor increase towards the boundaries of the integration domain, taking the unity value in the central part.

On the other hand, Figs. 1b, 2b and 3b display the considerable and progressive improvement of using the Fourier approximations to m^2 instead of the maximum value approximation in the domain, m_*^2. The size of the integration domain has been normalized so that in the tests results for different values of L_y can be compared.
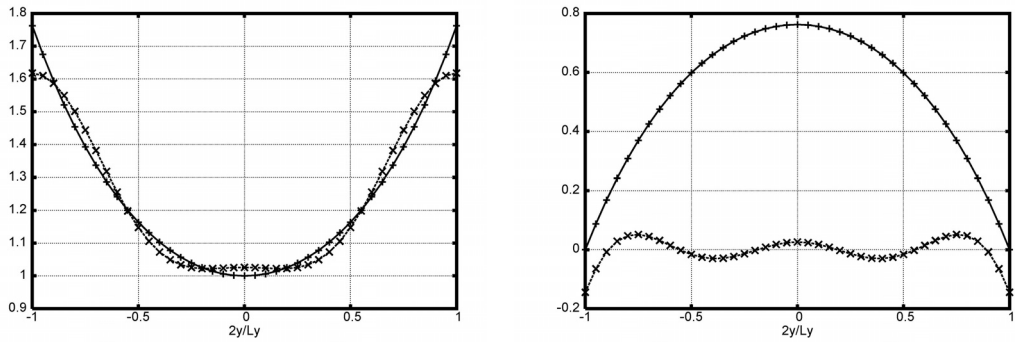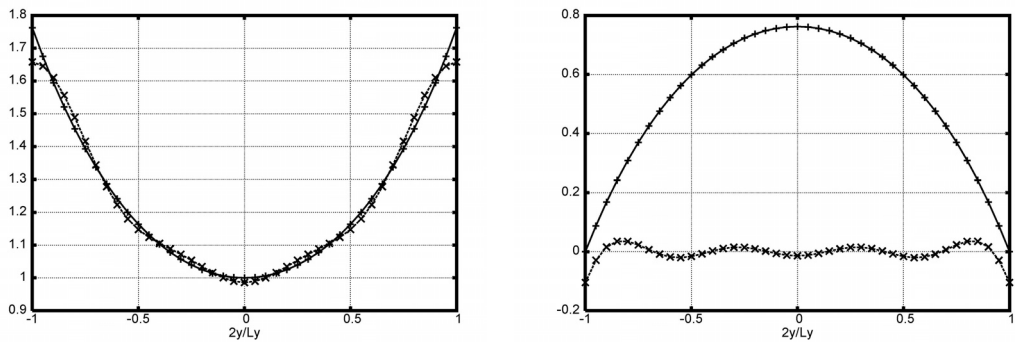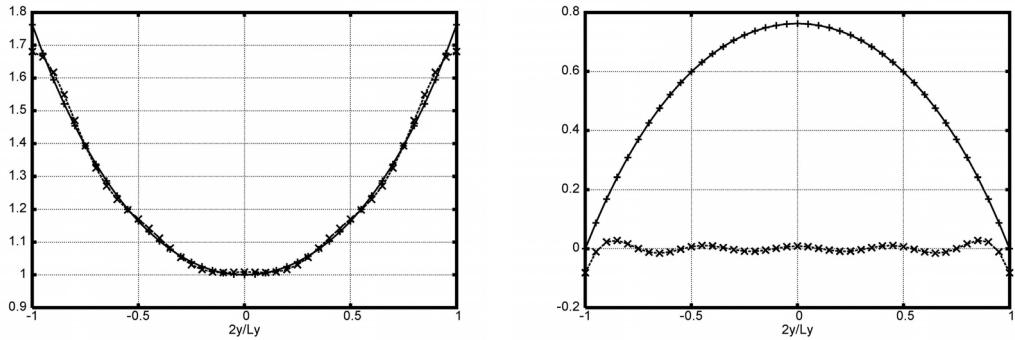
Figure 1. On the left, the square of the exact value of the map factor, in dots, and the square of the approximate value with coefficients: a_0, a_1 and a_2, in crosses. On the right, comparison of the Fourier approximation using coefficients: a_0, a_1 and a_2, in crosses, and the maximum approximation to the exact value, in dots. Ly=10050 km.

Figure 2. On the left, the square of the exact value of the map factor, in dots, and the square of the approximate value with coefficients: a_0, a_1, a_2 and a_3, in crosses. On the right, comparison of the Fourier approximation using coefficients: a_0, a_1, a_2 and a_3, in crosses, and the maximum approximation to the exact value, in dots. Ly=10050 km.

Figure 3. On the left, the square of the exact value of the map factor, in dots, and the square of the approximate value with coefficients: a_0, a_1, a_2, a_3 and a_4, in crosses. On the right, comparison of the Fourier approximation using coefficients: a_0, a_1, a_2, a_3 and a_4, in crosses, and the maximum approximation to the exact value, in dots. Ly=10050 km.

In the second test, the effect of the integration domain size is examined on both approximations to the exact value of m^2: the Fourier truncation with three coefficients and the square maximum value in the domain. To do this, four different sizes are considered:

$$L_y = 8375\,\text{km} \,(\, f = 1.3146\,), \ L_y = 6700\,\text{km} \,(\, f = 1.0516\,),$$
$$L_y = 5025\,\text{km} \,(\, f = 0.7887\,) \text{ and } L_y = 2512.5\,\text{km} \,(\, f = 0.3944\,)$$

Observing Figs. 1b and 4, it can be concluded that the greater the domain under study is, the better the Fourier truncation approximation of the map factor is in comparison with the maximum value approximation. However, when the size of the integration domain is smaller than 5000 km, the maximum value over the map factor area is a suitable approximation (Fig. 4d).
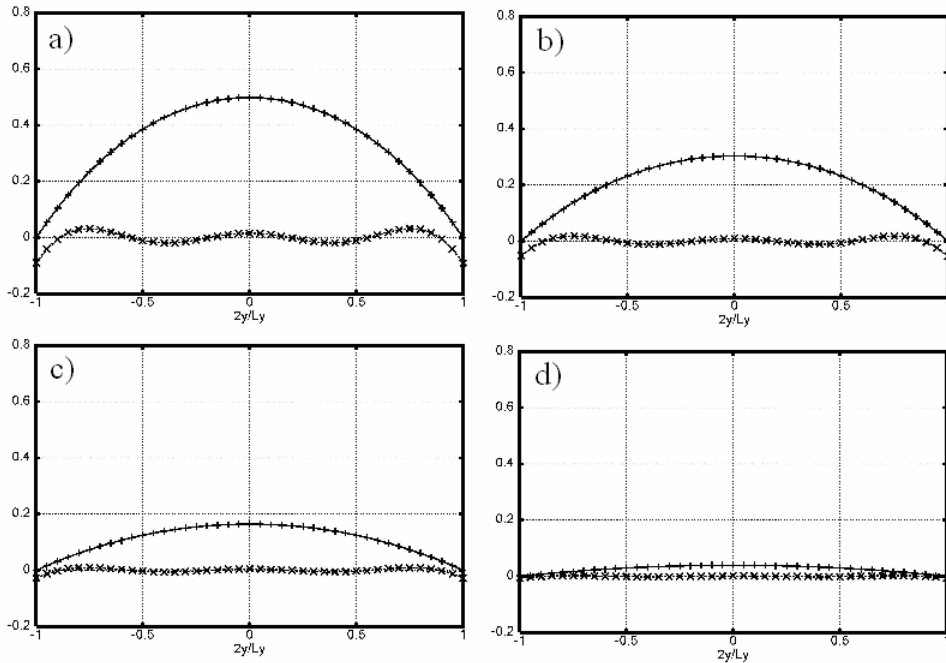
Figure 4. Comparison of the Fourier approximation to the exact value using coefficients: a_0, a_1 and a_2, in crosses, and the square maximum value approximation, in dots. a) Ly=8375 km, b) 6700 km, c) 5025 km and d) 2512.5 km.

5. FIRST RESULTS

Different test on the semi-Lagrangian integration have been submitted for the new semi-implicit scheme and for the original one at time-steps of 120, 300 and 900 seconds. Large domains, close to 6000 km in latitude, have been used to check the impact of the variable Mercator map factor.
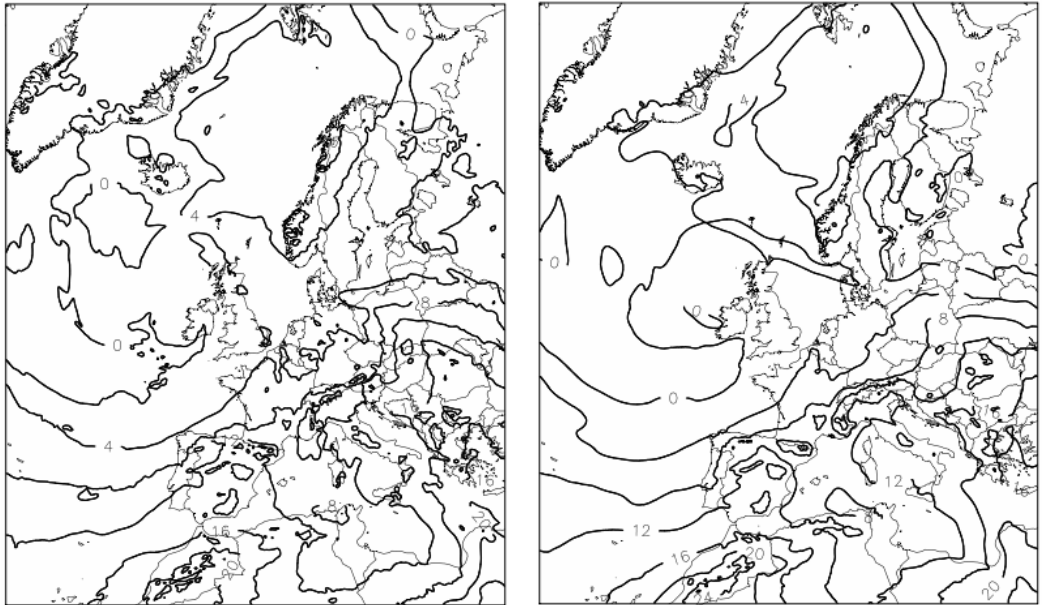
Figure 5. On the left, reference HARMONIE 48h forecast, with time-step of 900 seconds for the 850 hPa temperature field (in ºC). Initial situation: 14 May 2009, 12 UTC. On the right, reference HARMONIE analysis for 16 May 2009, 12 UTC.
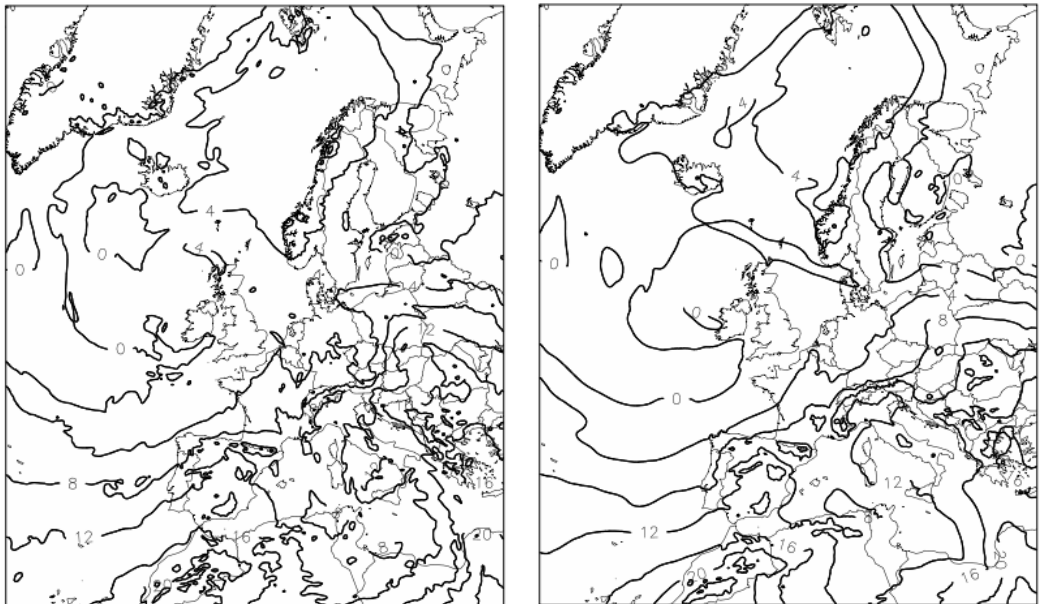

Figure 6. On the left, new HARMONIE 48h forecast, with time-step of 900 seconds for the 850 hPa temperature field (in ºC). Initial situation: 14 May 2009, 12 UTC. On the right, new HARMONIE analysis for 16 May 2009, 12 UTC.

Here, just the 850 hPa temperature field forecast after 48h for 900 second time-steps is shown. Figure 5 contains the results for the reference model and Fig. 6 shows the new semi-implicit scheme.

Comparing the results, small numerical differences among the new and reference schemes are found. Note that they specially appear at the central part of the domain.

Besides, it can be seen that both the reference and the modified scheme have some numerical noise. On the other hand, the non-hydrostatic version of the modified model could generate instabilities, as non-hydrostatic schemes are much more unstable in general. Following the steps of Yessad and Bénard (1996), the inclusion of a new geometrical term at the horizontal diffusion expression is under study, as it could solve both problems.

6. CONCLUSIONS

The main conclusions of this study can be summarized in the following points:
- The variability of the Mercator map factor should be considered for large domains.
- The analytical formula for the coefficients of the Fourier series of the rotated Mercator map factor has been obtained.
- The difference between using the Fourier approximation and the maximum value respect to the exact value of the map factor increases with the size of the integration domain.
- If the size of the integration domain is greater than 5000 km, the adjustment of the map factor by the first three coefficients of the Fourier series is much better than its maximum value over the area.
- The first results from the modified semi-implicit scheme look promising: more accurate than the obtained from the original one. However, further work is being developed in relation to the horizontal diffusion in order to ensure stability and to reduce noise in the fields.

7. ACKNOWLEDGEMENTS

APPENDIX

The general expression of the Fourier coefficients of the map factor in the cosine basis

$$cos(\frac{2\pi n}{L_y}y), \quad n = 0,1,2,...$$

is given by the formula:

$$a_n = \frac{4}{L_y}\int_0^{\frac{L_y}{2}} m^2(y)cos(\frac{2\pi n}{L_y}y)dy, \quad n = 0,1,2,...$$

where $L_y = fa$.

In this appendix, we obtain a simple expression for the Fourier coefficients of the Mercator map factor:

- <u>$n = 0$</u>

$$a_0 = \frac{4}{L_y}\int_0^{\frac{L_y}{2}} cosh^2(y)dy = \frac{4}{L_y}\int_0^{\frac{L_y}{2}} (\frac{e^{\frac{y}{a}}+e^{-\frac{y}{a}}}{2})^2 dy =$$

$$= \frac{4}{L_y}\int_0^{\frac{L_y}{2}} \frac{e^{\frac{2y}{a}}+e^{-\frac{2y}{a}}+2e^{\frac{y}{a}}e^{-\frac{y}{a}}}{4}dy = \frac{1}{L_y}\int_0^{\frac{L_y}{2}} (e^{\frac{2y}{a}}+e^{-\frac{2y}{a}}+2)dy =$$

$$= \frac{1}{L_y}[\frac{a}{2}e^{\frac{2y}{a}} - \frac{a}{2}e^{\frac{2y}{a}} + 2y]_{y=0}^{y=\frac{L_y}{2}} = \frac{1}{L_y}(\frac{a}{2}(e^{\frac{L_y}{a}} - e^{-\frac{L_y}{a}}) + L_y).$$

Replacing L_y by fa we get,

$$a_0 = \frac{1}{fa}(\frac{a}{2}(e^f - e^{-f}) + fa).$$

Then

$$a_0 = \frac{1}{2f}(e^f - e^{-f}) + 1.$$

- <u>$n \geq 1$</u>

$$a_n = \frac{4}{L_y}\int_0^{\frac{L_y}{2}} cosh^2(y)cos(\frac{2\pi n}{L_y}y)dy = \frac{4}{L_y}\int_0^{\frac{L_y}{2}} (\frac{e^{\frac{y}{a}}+e^{-\frac{y}{a}}}{2})^2 cos(\frac{2\pi n}{L_y}y)dy =$$

$$= \frac{4}{L_y} \int_0^{\frac{L_y}{2}} \frac{e^{\frac{2y}{a}} + e^{-\frac{2y}{a}} + 2e^{\frac{y}{a}}e^{-\frac{y}{a}}}{4} \cos(\frac{2\pi n}{L_y}y)dy = \frac{1}{L_y} \int_0^{\frac{L_y}{2}} (e^{\frac{2y}{a}} + e^{-\frac{2y}{a}} + 2)\cos(\frac{2\pi n}{L_y}y)dy.$$

This integral is divided in three integrals, corresponding to each one of the additions, respectively.

- **(I)**

$$(I) = \int_0^{\frac{L_y}{2}} e^{\frac{2y}{a}} \cos(\frac{2\pi n}{L_y}y)dy.$$

Applying integration by parts:

$$(I) = [\frac{L_y}{2\pi n}e^{\frac{2y}{a}} sen(\frac{2\pi n}{L_y}y)]_{y=0}^{y=\frac{L_y}{2}} - \int_0^{\frac{L_y}{2}} \frac{L_y}{2\pi n}sen(\frac{2\pi n}{L_y}y)\frac{2}{a}e^{\frac{2y}{a}}dy =$$

$$= [\frac{L_y}{2\pi n}e^{\frac{2y}{a}} sen(\frac{2\pi n}{L_y}y)]_{y=0}^{y=\frac{L_y}{2}} - \int_0^{\frac{L_y}{2}} \frac{f}{\pi n}e^{\frac{2y}{a}} sen(\frac{2\pi n}{L_y}y)dy.$$

Using integration by parts again:

$$(I) = [\frac{L_y}{2\pi n}e^{\frac{2y}{a}} sen(\frac{2\pi n}{L_y}y) + \frac{fL_y}{2n^2\pi^2}e^{\frac{2y}{a}} cos(\frac{2n\pi}{L_y}y)]_{y=0}^{y=\frac{L_y}{2}} - \frac{f^2}{(n\pi)^2}\int_0^{\frac{L_y}{2}} e^{\frac{2y}{a}} cos(\frac{2n\pi}{L_y}y)dy =$$

$$= [\frac{L_y}{2\pi n}e^{\frac{2y}{a}} sen(\frac{2\pi n}{L_y}y) + \frac{fL_y}{2n^2\pi^2}e^{\frac{2y}{a}} cos(\frac{2\pi L_y}{2n^2\pi^2}e^{\frac{2y}{a}} cos(\frac{2\pi n}{L_y}y)]_{y=0}^{y=\frac{L_y}{2}} \frac{f^2}{(\pi n)^2}(I).$$

Then,

$$[1+(\frac{f}{\pi n})^2](I) = \frac{L_y}{2\pi n}[\frac{f}{\pi n}e^f cos(\pi n) - \frac{f}{\pi n}].$$

And finally,

$$(I) = [\frac{L_y}{2\pi n}((-1)^n \frac{f}{\pi n}e^f - \frac{f}{\pi n})]/[1+(\frac{f}{\pi n})^2].$$

- **(II)**

$$(II) = \int_0^{\frac{L_y}{2}} e^{-\frac{2y}{a}} cos(\frac{2\pi n}{L_y} y) dy.$$

Applying also integration by parts:

$$(II) = [\frac{L_y}{2\pi n} e^{-\frac{2y}{a}} sen(\frac{2\pi n}{L_y} y)]_{y=0}^{y=\frac{L_y}{2}} + \int_0^{\frac{L_y}{2}} \frac{f}{\pi n} e^{-\frac{2y}{a}} sen(\frac{2\pi n}{L_y} y) dy.$$

Using integration by parts again:

$$(II) =$$

$$= [\frac{L_y}{2\pi n} e^{-\frac{2y}{a}} sen(\frac{2\pi n}{L_y} y) - \frac{fL_y}{2n^2\pi^2} e^{-\frac{2y}{a}} cos(\frac{2\pi n}{L_y} y)]_{y=0}^{y=\frac{L_y}{2}} - \frac{f^2}{(n\pi)^2} \int_0^{\frac{L_y}{2}} e^{-\frac{2y}{a}} cos(\frac{2n\pi}{L_y} y) dy =$$

$$= [\frac{L_y}{2\pi n} e^{-\frac{2y}{a}} sen(\frac{2\pi n}{L_y} y) - \frac{fL_y}{2n^2\pi^2} e^{-\frac{2y}{a}} cos(\frac{2\pi L_y}{2n^2\pi^2} e^{-\frac{2y}{a}} cos(\frac{2\pi n}{L_y} y)]_{y=0}^{y=\frac{L_y}{2}} \frac{f^2}{(\pi n)^2} (II).$$

Then, we obtain:

$$(II) = [\frac{L_y}{2\pi n}(-(-1)^n \frac{f}{\pi n} e^{-f} + \frac{f}{\pi n})]/[1+(\frac{f}{\pi n})^2].$$

- **(III)**

Lastly,

$$(III) = \int_0^{\frac{L_y}{2}} cos(\frac{2\pi n}{L_y} y) dy = [\frac{L_y}{2\pi n} sen(\frac{2\pi n}{L_y} y)]_{y=0}^{y=\frac{L_y}{2}} = \frac{L_y}{2\pi n} sen(n\pi) = 0.$$

Replacing the expressions (I), (II) and (III) in a_n, we deduce:

$$a_n = \frac{1}{2\pi n}((-1)^n \frac{f}{\pi n} e^f - (-1)^n \frac{f}{\pi n})/(1+(\frac{f}{\pi n})^2)$$

$$a_n = \frac{(-1)^n f}{2((\pi n)^2 + f^2)}(e^f - e^{-f}).$$

8. REFERENCES

BÉNARD, P. (2003). *Scientific Documentation for Aladin-NH Dynamical Kernel* (version 2.0), http://www.cnrm.meteo.fr:80/gmapdoc/spip.php?article21, Chapter 3, Associated Linear Continuous System, pp. 22-32, 81 pp.

BÉNARD, P. (2004). *New ``Rotated/Tilted Mercator" geometry in Aladin*, http://www.cnrm.meteo.fr/gmapdoc/spip.php?article53&var_recherche=%22Rotated%20Tilted%20Mercator%20geometry%20in%20aladin%22&var_lang=en, 20 pp.

VOITUS, F. (2004). *Liens entre la geometrie horizontale et le schema semi-implicite dans les modeles Arpege, Arpege/Aladin, et Arpege/Aladin-NH*, Rapport de stage de fin d'études nº951, Ecole Nationale de la Météorologie.

YESSAD, K & P. BÉNARD (1996). Introduction of a local mapping factor in the spectral part of the Météo-France global variable mesh numerical forecast model, *Quart. J. Roy. Meteor. Soc.*, 122, 1701-1719.